Journal of Power Sources 188 (2009) 319–322

Contents lists available at ScienceDirect

Journal of Power Sources

journal homepage: www.elsevier.com/locate/jpowsour

Short communication

Preparation of polymer film of micro-porous or island-like structure and its application in dye-sensitized solar cell

Chih-Ming Chen[a,*], Han-Sheng Shiu[a], Sheng-Jye Cherng[a], Tzu-Chien Wei[b]

[a] Department of Chemical Engineering, National Chung-Hsing University, Taichung 402, Taiwan
[b] Department of Chemical Engineering, National Tsing-Hua University, Hsin-Chu 300, Taiwan

ARTICLE INFO

Article history:
Received 1 October 2007
Received in revised form 7 October 2008
Accepted 8 October 2008
Available online 24 November 2008

Keywords:
Polymers
Solar cells
Structural properties
Surface morphology

ABSTRACT

A polystyrene (PS) film of micro-porous or island-like structure has been prepared by spin-coating the PS–PMMA (polymethyl-methacrylate) blend on sputtered platinum electrode, followed by selectively dissolving PMMA out of the blend. The film forms either micro-porous or island-like structure depending on the blending proportion of PS to PMMA. After soaking with liquid electrolyte, this film can be utilized as gel polymer electrolyte for dye-sensitized solar cell to improve its durability because the evaporation rate of liquid electrolyte can be significantly reduced. As to the convenience of cell assembly, this polymer film can also serve as a spacer and effectively separate the photo-anode and counter electrode. In addition, we also find that the cell performance is affected significantly by the polymer blend concentration. An energy conversion efficiency of 4.58% can be obtained with 2 wt% PS–2 wt% PMMA blend proportion under AM 1.5, 1 Sun illumination.

1. Introduction

Solar cell is a device that converts solar power into electricity directly and is regarded as one of the most potential candidates to provide alternative energy. Among various solar cell systems, dye-sensitized solar cell (DSSC) introduced by Grätzel and co-workers [1–5] possesses many advantages, such as low cost, easy assembly, and high energy conversion efficiency. Although DSSC has been developed successfully and ready to enter a level of commercial application, some reliability issues still needs to be solved, such as leakage and dry-out of liquid electrolytes under sunlight illumination [6]. The liquid electrolyte usually contains volatile organic solvents serving as a transport media for redox couple species. Once the cell is sealed improperly, the solvents might vaporize and the electrolyte would dry up. To solve this issue and improve the long-term durability of DSSC, extensive efforts are devoted on using different types of charge transport materials, such as polymer gel [7–14], ion liquid [15–17], organic [18–20], or inorganic p-type semiconductors [21,22], to replace the volatile solvent. However, the cell usually encounters significant performance loss due to lower charge transport nature of these substitutions.

In this study, we prepare a solid polymer film directly on the counter electrode before cell assembly. The film contains ample micro-pores or free space which can absorb or fill the liquid electrolyte. In addition, due to the immiscibility between polymer film and liquid electrolyte, it can remain as solid structure on the surface of counter electrode. Consequently, both of proper mechanical strength of the solid film and good ionic conductivity of liquid electrolyte can be obtained simultaneously. More importantly, the film can effectively absorb the liquid electrolyte and reduce its evaporation rate significantly. Another advantage is that the film is spin-coated on the overall surface of the counter electrode; it functions like a spacer which can effectively separate the photo-anode and counter electrode. Thus, the cell assembly procedure becomes simple and reliable because the possibility of short-circuit failure can be significantly lowered in this system.

2. Experimental procedures

2.1. Preparation and examination of polymer films

In this study, two polymers, polystyrene (PS, MW = 280,000) and polymethyl-methacrylate (PMMA, MW = 120,000), were used as obtained. Each polymer was dissolved in methyl ethyl ketone (MEK) to prepare the homogeneous polymer solution of different concentrations. Then the PS and PMMA solutions of equal volume were mixed to prepare the binary PS–PMMA blend solution. The concentrations of the homogeneous PS or PMMA solution and the mixing proportions are listed in Table 1. Mirror-like sputtered platinum on indium tin oxide (Pt/ITO) glass serving as substrate was cleaned in supersonic bath and dried by nitrogen jet before use.

* Corresponding author. Tel.: +886 422859458; fax: +886 422854734.
E-mail address: chencm@nchu.edu.tw (C.-M. Chen).

0378-7753/$ – see front matter © 2008 Elsevier B.V. All rights reserved.
doi:10.1016/j.jpowsour.2008.10.138

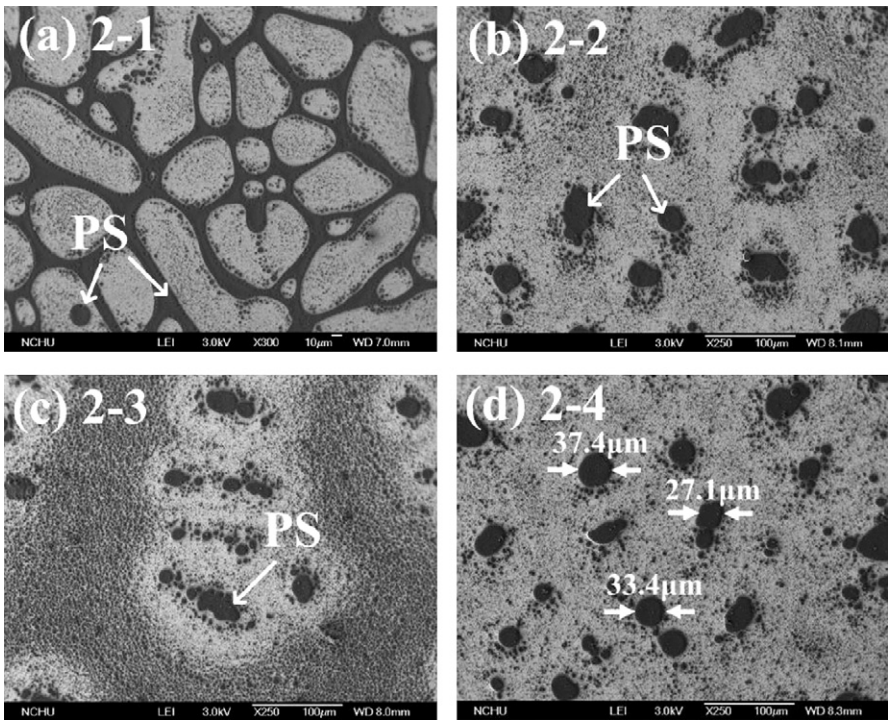

Fig. 1. SEM images of the polymer films after the removal of the PMMA phase: (a) 2 wt% PS–1 wt% PMMA, (b) 2 wt% PS–2 wt% PMMA, (c) 2 wt% PS–3 wt% PMMA, and (d) 2 wt% PS–4 wt% PMMA.

PS–PMMA film was spin-coated on Pt/ITO glass by dipping 0.2 ml polymer solution onto the surface at 300 rpm for 60 seconds until a uniform PS–PMMA film was formed. The wet PS–PMMA film was placed in air for 48 h to evaporate the MEK solvent. The solvent-free film was immersed in acetic acid for 72 h to completely dissolve PMMA out of the PS–PMMA blend film. Field-emission scanning electron microscopy (FE-SEM) was used to examine the surface morphology of the polymer film. Film thickness was measured by scanning through the polymer film down to the electrode using alpha-step.

2.2. Testing of evaporation rates

To monitor the evaporation rate, the PS-coated Pt/ITO glass was first dipped into liquid electrolyte (0.6 M DMPII, 0.1 M LiI, 0.05 M iodine, and 0.5 M TBP (4-tert-butylpyridine) in 3-MPN) for 1 h to soak liquid electrolyte completely. Then the weight loss of the wet film was recorded under atmosphere exposure. For comparison, the weight loss rate of liquid electrolyte on a polymer-free Pt/ITO glass was also measured as a reference.

Table 1
Film thickness as a function of concentrations of the PS–PMMA blend.

PS–PMMA (wt%)	Film thickness (μm)
2–1	1.05
2–2	1.66
2–3	1.71
2–4	2.18
3–1	1.26
3–2	1.57
3–3	2.48
3–4	2.89
4–1	1.74
4–2	2.52
4–3	3.66
4–4	3.89

2.3. Cell assembly and testing

A TiO_2 photo-anode (Dyesol, Australia) was sintered at 500 °C for 30 min and then immersed in an ethanol solution of 0.4 mM N719 dye for 12 h. After dye-coating, the photo-anode was assembled with wet PS-covered counter electrode. For comparison, a conventional liquid electrolyte-based DSSC was also fabricated by employing a thermoplastic film (25 μm, SX-1170-25, Solaronix) as the spacer. Cell performance was evaluated under AM 1.5, 1 Sun illumination with a solar simulator (Newport). Photocurrent–voltage (*I–V*) curves were recorded using a computer-controlled digital source meter (Keithley, model 2400). The active area of the cell was 0.28 cm^2.

3. Results and discussion

3.1. Morphology of polymer films

Fig. 1 shows the SEM images of the polymer blend films after the removal of the PMMA phase. In Fig. 1(a)–(d), the PS concentration of the as-blended polymer film is fixed at 2 wt% while the PMMA concentration increases from 1 to 4 wt%. As shown in Fig. 1(a) for 1 wt% PMMA concentration, the film presents a network structure with many pores inside. The pore size ranges from few to hundreds of micrometers. There are plenty of small island-like PS phase inside the pores. When PMMA addition increases over 2 wt%, the network structure disappears and is replaced by a large number of island-like PS phase as shown in Fig. 1(b)–(d).

Obviously, the concentration proportion of PS to PMMA in the polymer blend has significant effects on the film morphology. The PS phase acts as a continuous network matrix when its concentration is higher than PMMA. In the film of 2 wt% PS–1 wt% PMMA proportion as shown in Fig. 1(a), phase separation of PS and PMMA takes place after solvent evaporation since these two polymers are immiscible. By selectively removing PMMA, pores are formed and a PS film of continuous network structure is created. However,

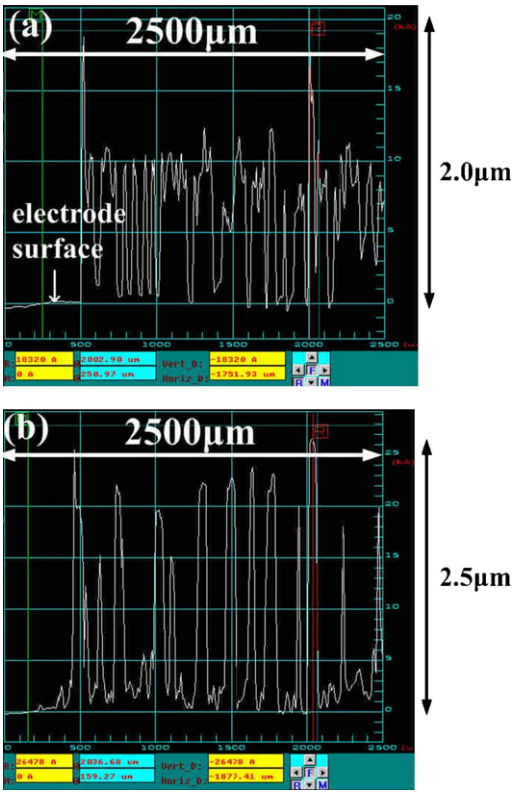

Fig. 2. Scanning topography of the polymer film using alpha-step: (a) 2 wt% PS–1 wt% PMMA and (b) 2 wt% PS–4 wt% PMMA.

when the PS concentration is lower than PMMA, PMMA transforms into the continuous matrix phase and PS turns into discontinuous island-like structure. Therefore, as shown in Fig. 1(b)–(d), island-like PS phase is created after PMMA is selectively removed. Similar morphology was also observed in the 3 and 4 wt% PS film.

Surface morphologies of the polymer films shown in Fig. 1 were also analyzed using alpha-step profile meter. The scanning topography is shown in Fig. 2, where Fig. 2(a)–(b) represent the 2 wt% PS–1 wt% PMMA and 2 wt% PS–4 wt% PMMA proportions, respectively. The film thicknesses can be measured from Fig. 2 and are listed in Table 1. For the PS concentration fixing at 2 wt%, the film thickness increases with more PMMA blending. Similar results were also found in the polymer blend containing 3 and 4 wt% PS as listed in Table 1. The increment of film thickness with increasing polymer concentration is due to the viscosity increment of the polymer solution. The polymer solution becomes more viscous when the polymeric concentration increases. The spread ability of the polymer solution during spin-coating becomes poor, and thus a thicker film is formed. Additionally, in Fig. 2 the pore density decreases but the pore size increases with increasing PMMA concentration. Most of the pores extend from the air to the underlying electrode surface. Similar results were also found in the other PS–PMMA proportions.

3.2. Effects of polymer film on evaporation rates of liquid electrolytes

Fig. 3 shows the rate of weight loss of liquid electrolyte in the 2 wt% PS film. The symbol "2–1" represents 2 wt% PS–1 wt% PMMA, "2–2" represents 2 wt% PS–1 wt% PMMA, and so forth. The data of pure liquid electrolyte on counter electrode are also plotted in Fig. 3 for comparison. Generally, any weight loss measured in this study should be ascribed to the evaporation of the organic solvent, because all other components in the cell have negligible vapor pressure under atmospheric condition. Obviously, compared to pure

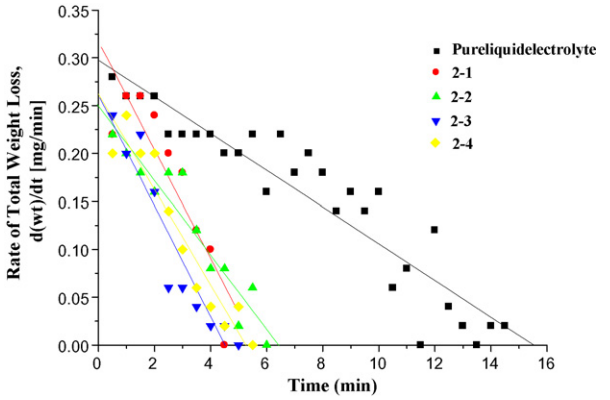

Fig. 3. Rate of weight loss of liquid electrolyte in the 2 wt% PS film as a function of exposure time.

liquid electrolyte, the rate of weight loss of liquid electrolyte in the electrode covered with a polymer film is slower at any testing times and decreases in a quicker manner. Similar results were also observed in the 3 and 4 wt% PS films. Based on the above results, utilizing a polymer film with porous or island-like structure in DSSC can effectively improve the solvent retention in liquid electrolyte, and thus slows down its evaporation rate. This could be explained by the "absorbability" of the polymer film to liquid electrolyte. As shown in Fig. 1, the polymer films contain a large number of pores and free space that can fill liquid electrolyte. Therefore, the liquid electrolyte can be absorbed more closely in the polymer film and its evaporation rate can be slowed down.

3.3. Cell efficiency

The photocurrent–voltage (I–V) curves of the DSSC employing a 2 wt% PS film are shown in Fig. 4, where the data of a conventional DSSC without a polymer film are also plotted for comparison (labeled as "pure liquid electrolyte"). Cell efficiency can be obtained from Fig. 4 and are listed in Table 2. It can be found that the 2 wt% PS films ("2–1" to "2–4") show better efficiency (η) performance that can exceed 4%, in which the polymer film with 2 wt% PS–2 wt% PMMA proportion exhibits a highest efficiency, 4.58%, among all polymeric proportions. Compared to the conventional DSSC without a polymer film (η = 4.62%), the efficiency merely drops 0.04%. The efficiencies of the 3 wt% PS films are around 3.3–4%. The 4 wt% PS films exhibit lower efficiencies which are around 2%. Obviously, the higher the polymeric concentration is, the lower the cell efficiency.

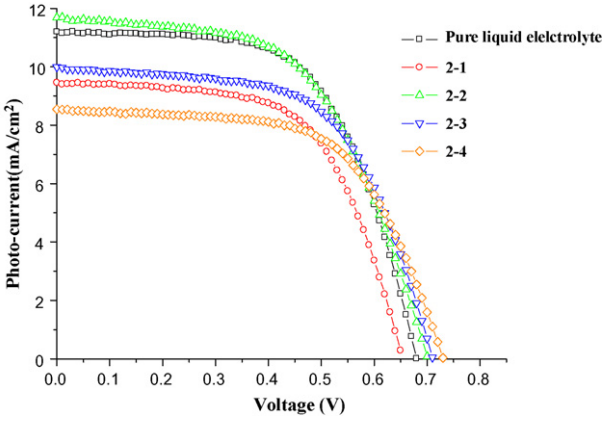

Fig. 4. Photocurrent–voltage (I–V) curves of DSSC employing a polymer film.

Table 2
Cell performances as a function of concentrations of the PS–PMMA blend.

PS–PMMA (wt%)	V_{OC} (V)	I_{SC} (mA/cm^2)	FF (fill factor)	η (%)
Pure liquid electrolyte	0.68	11.19	0.61	4.62
2–1	0.65	9.45	0.61	3.75
2–2	0.70	11.68	0.56	4.58
2–3	0.71	9.98	0.60	4.24
2–4	0.73	8.54	0.61	3.82
3–1	0.68	9.54	0.58	3.78
3–2	0.69	9.82	0.58	3.97
3–3	0.73	8.08	0.59	3.53
3–4	0.76	7.23	0.61	3.32
4–1	0.72	6.16	0.47	2.09
4–2	0.72	5.14	0.54	2.00
4–3	0.79	4.03	0.60	1.89
4–4	0.76	4.45	0.61	2.09

It is now acknowledged that the electrolyte evaporation and leakage is one of the main factors that decrease DSSC durability. Polymer gel electrolytes with better solvent-preservation have been introduced to increase its durability. But this replacement would lead to degradation of charge transport ability and lower the cell efficiency significantly. So, the target to reach high efficiency and low volatility seems to be in a dilemma. In this study, we propose a compromising method as discussed above by sandwiching a solid polymer film in between two electrodes. Since the polymer film is formed directly on the counter electrode, the cell assembly procedure becomes simple and the short circuiting concern of the cell can be neglected. The structure of this film is either porous or island-like. So, there are plenty of pores and free space inside this film which can absorb (or fill) liquid electrolyte effectively. Since the solid polymer film is immiscible with the liquid electrolyte, the electrolyte can remain as liquid and thus provide a good ionic conductivity. More importantly, as discussed in Section 2.2, the polymer film can effectively reduce the evaporation rate of liquid electrolyte. Additionally, due to a solid structure, the polymer film should be able to serve as a spacer, and can promote the mechanical property of DSSC.

Although the electrolyte can function as liquid phase, the transporting performance of iodine ions should still degrade due to the presence of a non-conductive polymer film. However, as discussed above, the DSSC employing 2 wt% PS–2 wt% PMMA polymer film shows a comparable efficiency to the conventional DSSC. We believe that this effect should be ascribed to the thinner thickness of the polymer film. In conventional DSSC, due to the usage of a thermoplastic spacer, the distance between photo-anode and counter electrode is about 25 μm. However, the distance between photo-anode and counter electrode in DSSC studied here is shortened greatly because the thermoplastic spacer is replaced by a thinner polymer film. As listed in Table 2, the film thickness is only 1.66 μm which is far smaller than 25 μm. With a shorter distance, the time needed for ion diffusion between photo-anode and counter electrode can be shorten. This advantage seems to be able to compensate the degradation of ionic conductivity, and consequently the cell efficiency can be kept. However, the cell efficiency will drop when the polymer concentrations increases as shown in Table 2. This concentration effect can also be explained on the basis of film thickness. As shown in Table 1, higher polymer concentration corresponds to a thicker film, and consequently the cell efficiency decreases with increasing polymer concentration. The effect of distance between photo-anode and counter electrode (spacer thickness) on the cell performance was also investigated previously [23,24]. Similar results were also obtained for the DSSCs employing liquid or ionic liquid electrolyte, that is, energy conversion efficiency was decreased as the distance between two electrodes was increased.

4. Conclusions

A PS polymer film of micro-porous or island-like structure can be prepared by spin-coating the PS–PMMA blend of different concentrations on sputtered platinum electrode, followed by selectively removing the PMMA phase out of the blend. This film can be spin-coated on the counter electrode of DSSC before cell assembly, which can be used as a spacer to effectively separate the photo-anode and counter electrode. Thus, short-circuit failure due to contact of the two electrodes can be prevented. Additionally, this film can improve the solvent retention in DSSC by absorbing (or keeping) liquid electrolyte inside the pores or free spaces of the film. Evaluation of cell performances shows efficiency drop when the PS film is employed in DSSC. The degree of efficiency drop depends on the film thickness. For the 2 wt% PS–2 wt% PMMA blend, the film thickness is only 1.66 μm, and a negligible efficiency drop (only 0.04%) can be achieved. This polymer film should also have high potentials in the application of flexible DSSC, since this film can be also used as a spacer to prevent short-circuit due to cell bending or deformation. Investigation will be conducted in near future to survey the feasibility of the PS film on flexible substrate.

Acknowledgements

The authors wish to acknowledge the financial support of National Science Council of Taiwan, ROC through Grant NSC 96-ET-7-005-001-ET. This work is supported in part by the Ministry of Education, Taiwan, R.O.C. under the ATU plan.

References

[1] B. O'Regan, M. Grätzel, Nature 353 (1991) 737.
[2] M.K. Nazeeruddin, A. Kay, I. Rodicio, R. Humphry-Baker, E. Müller, P. Liska, N. Vlachopoulos, M. Grätzel, J. Am. Chem. Soc. 115 (1993) 6382.
[3] M. Grätzel, Nature 414 (2001) 338.
[4] M. Grätzel, J. Photochem. Photobiol. C 4 (2003) 145.
[5] M. Grätzel, J. Photochem. Photobiol. A 164 (2004) 3.
[6] N. Papageorgiou, W.F. Maier, M. Grätzel, J. Electrochem. Soc. 144 (1997) 876.
[7] S.R. Scully, M.T. Lloyd, R. Herrera, E.P. Giannelis, G.G. Malliaras, Synth. Mater. 144 (2004) 291.
[8] P. Wang, S.M. Zakeeruddin, J.E. Moser, M.K. Nazeeruddin, T. Sekiguchi, M. Grätzel, Nat. Mater. 2 (2003) 402.
[9] S. Sakaguchi, H. Ueki, T. Kado, R. Shiratuchi, W. Takashima, K. Kaneto, S. Hayase, J. Photochem. Photobiol. A 164 (2004) 117.
[10] D.W. Kim, Y.B. Jeong, S.H. Kim, D.Y. Lee, J.S. Song, J. Power Sources 149 (2005) 112.
[11] R. Komiya, L. Han, R. Yamanaka, A. Islam, T. Mitate, J. Photochem. Photobiol. A 164 (2004) 123.
[12] D. Saikia, C.C. Han, Y.W. Chen-Yang, J. Power Sources 185 (2008) 570.
[13] M.S. Kanga, K.S. Ahnb, J.W. Lee, J. Power Sources 180 (2008) 896.
[14] J.Y. Kim, T.H. Kim, D.Y. Kim, N.G. Park, K.D. Ahn, J. Power Sources 175 (2008) 692.
[15] P. Wang, S.M. Zakeeruddin, R. Humphry-Baker, M. Grätzel, Chem. Mater. 16 (2004) 2694.
[16] P. Wang, S.M. Zakeeruddin, J.E. Moser, M. Grätzel, J. Phys. Chem. B 107 (2003) 13280.
[17] V. Jovanoski, E. Stathatos, B. Orel, P. Lianos, Thin Solid Films 511–512 (2006) 634.
[18] U. Bach, D. Lupo, P. Comte, J.E. Moser, F. Wiessörtel, J. Salbeck, H. Spreitzer, M. Grätzel, Nature 395 (1998) 583.
[19] D. Gebeyehu, C.J. Brabec, N.S. Sariciftci, Thin Solid Films 403 (2002) 271.
[20] J.H. Park, K.J. Choi, S.W. Kang, Y.S. Kang, J. Kim, S.S. Lee, J. Power Sources 183 (2008) 812.
[21] B. O'Regan, F. Lenzmann, R. Muis, J. Wienke, Chem. Mater. 14 (2002) 5023.
[22] G.R.A. Kumara, S. Kaneko, M. Okuya, K. Tennakone, Langmuir 18 (2002) 10493.
[23] H. Matsui, K. Okada, T. Kawashima, T. Ezure, N. Tanabe, R. Kawano, M. Watanabe, J. Photochem. Photobiol. A 164 (2004) 129.
[24] T. Hoshikawa, M. Yamada, R. Kikuchi, K. Eguchi, J. Electroanal. Chem. 577 (2005) 339.